

# Design of a co-integrated CMOS/NEMS oscillator with a simple electronic circuit

Gregory Arndt\*, Eric Colinet\*, Jerome Juillard<sup>+</sup>

\*CEA-LETI MINATEC, <sup>+</sup>SUPELEC

<sup>\*</sup>17 rue des Martyrs, 38054 Grenoble Cedex 09, France

<sup>+</sup>3, rue Joliot-Curie, 91192 Gif-sur-Yvette Cedex, France

Tel.: +00-33-4-38-78-17-53, fax: +00-33-4-38-78-24-34, email: eric.colinet@cea.fr

**Abstract**-This paper presents the theoretical study of a monolithically integrated NEMS/CMOS oscillator with electrostatic actuation and piezoresistive detection. A feedback circuit based on a single active transistor is implemented. The proposed architecture is so compact that it can be implemented with ease in a sensor array application for example. A brief description of the NEMS resonator is given and the conditions for oscillation build-up are stated. We show how the co-integration allows the use of a very simple sustaining electronic circuit. This paper focuses on the determination of the system steady-state and more specifically the amplitude of the mechanical displacement and electronic output voltage. We show that the intrinsic nonlinearities of the electronic circuit can be used to achieve stable oscillation. The proposed oscillator exhibits a large output signal while keeping small mechanical amplitude compared to the electrostatic gap.

## I. INTRODUCTION

NEMS (NanoElectroMechanical Systems) resonators used as sensors feature great advantages in terms of performance, cost, and compactness. They can potentially be applied in a wide range of domains: chemistry, biomedical sensors, mobile electronic devices. NEMS are often used as resonant sensors. In order to track their resonance frequency, one approach consists in embedding the NEMS in a self-oscillating loop. Such oscillators are composed of a NEMS resonator and a feedback electronic. Advantages of this detection scheme are their simple electronics compared to other architectures [1], their fast responsivity and their large dynamic range [2]. When it is technologically feasible, integrating the resonator and its electronic very close (ideally on the same wafer) increases the Signal-to-Noise Ratio (SNR) and simplifies the electronic feedback circuit [3-5].

This paper describes the design of a co-integrated oscillator based on a resonator whose fabrication is compatible with CMOS-processes. This resonator uses electrostatic actuation and piezoresistive detection. The electronic circuit is very simple, based on a single active transistor. The control of the oscillation amplitude is achieved through the intrinsic nonlinearities of the electronics rather than through an automatic gain control (AGC) [6]. Determination of the steady-state oscillation amplitude is achieved thanks to the describing function (DF) method [7]. DF is a particular case of the harmonic balance method where only the fundamental harmonic is

considered. The knowledge of the electronic behavior together with that of the NEMS transfer function makes it possible to determine the steady state of the whole system.

In section II, the NEMS resonator and its model are presented. The oscillation conditions and the constraints imposed on the sustaining electronic are stated and the design of the electronic circuit is also addressed. The qualitative behavior of the oscillator and the characteristics of its steady-state regime are determined in section III. These results are validated by transient simulations of the complete closed-loop system.

## II. DESCRIPTION OF THE NEMS OSCILLATOR

### A. Model of the mechanical resonator

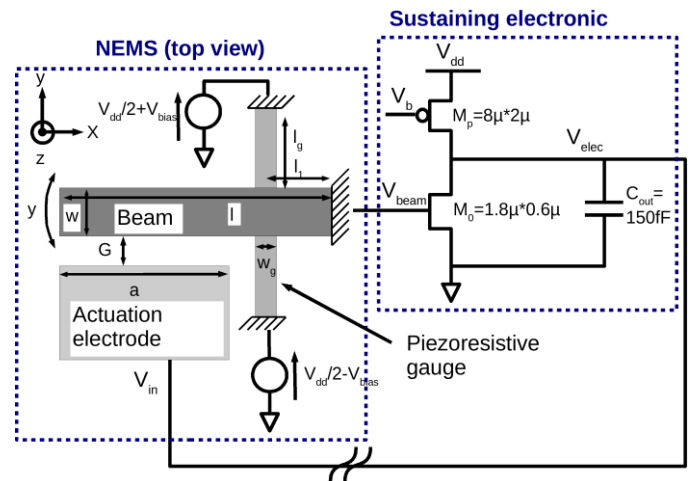


Fig. 1. Architecture of the proposed NEMS/CMOS oscillator.

Fig. 1 shows the oscillator composed of the NEMS resonator and its feedback electronic circuit. The NEMS is actuated using electrostatic forces and its displacement is detected using the piezoresistive gauges presented in [8]. The voltage applied upon the actuation electrode is converted into an in-plane mechanical motion  $y$  of the beam. The displacement of the beam is assumed to be unimodal. It is characterized by its modal mass  $m_e$  and its natural pulsation  $\Omega_1$ . The variation induced in the resistance gauge is converted into a charge modulation by properly

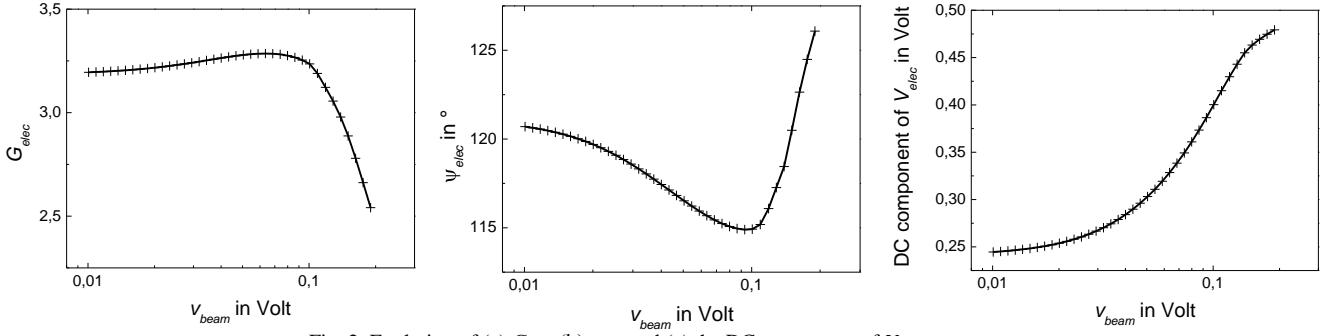


Fig. 2. Evolution of (a)  $G_{elec}$ , (b)  $\psi_{elec}$  and (c) the DC component of  $V_{elec}$  versus  $v_{beam}$ .

polarizing the bridge configuration shown in figure 1. The NEMS has the following dimensions:  $2\mu\text{m}$  long ( $l$ ),  $100\text{nm}$  wide ( $w$ ) and  $40\text{nm}$  thick ( $t$ ). The actuation electrode is  $1.6\mu\text{m}$  long ( $a$ ) and is separated from the beam by a gap of  $100\text{nm}$  ( $G$ ). The gauges are  $250\text{nm}$  long ( $l_g$ ),  $40\text{nm}$  wide ( $w_g$ ) and  $40\text{nm}$  thick ( $t$ ). The expected quality factor ( $Q$ ) of this device in vacuum is 1000 [8]. Due to the nanometric size of the gauges section, the piezoresistive effect is supposed to be giant [9] and its expected piezoresistive factor to be  $\gamma_L=2000$ . According to the given dimensions,  $\Omega_1 \approx 2\pi \times 50\text{MHz}$ .

The following notations are used:  $V_{in}$  is the voltage applied to the actuation electrode and  $V_{beam}$  is the voltage of the beam (see fig. 1).  $v_{in}$  and  $v_{beam}$  are respectively their AC components with pulsation  $\omega$ .  $V_{DC}$  is the DC component of  $V_{beam}-V_{in}$ .

Assuming that the mechanical displacement of the beam is negligible compared to the gap, i.e.  $y \ll G$ , the AC component of the electrostatic actuation force is:

$$F = \frac{C_0 V_{DC}}{G} v_{in}, \quad (1)$$

where  $C_0 = \epsilon_0 a t / G$  is the static capacitance of the actuation electrode and  $\epsilon_0$  is the permittivity of vacuum.

The NEMS motion-input voltage transfer function  $\alpha(\omega)$  can be expressed as [8]:

$$\alpha(\omega) = \frac{y}{v_{in}} = \frac{C_0 V_{DC} / G}{m_e \left( \Omega_1^2 - \omega^2 + j \frac{\omega \Omega_1}{Q} \right)}. \quad (2)$$

The relative change of the gauge resistance is [8]:

$$\frac{\Delta R}{R_0} = \gamma_L \frac{A_1 I}{t w_g} y, \quad (3)$$

where  $A_1 = 1.31 \times 10^{-19}$  is a constant that depends on the boundary, the normalization conditions and the excitation mode,  $I$  is the moment of inertia of the beam,  $R_0 = \rho l_g / (w_g t)$  is the resistance of the gauge and  $\rho = 8.8 \mu\Omega \cdot \text{m}$  is the resistivity of the gauge (corresponding to a doping level of  $10^{19} \text{cm}^{-3}$ ).

Assuming that the input impedance of the electronic circuit is large compared to  $R_0$ , the NEMS resonator and its detection can be modeled as follows:

$$H_{nems}(\omega) = \frac{v_{beam}}{v_{in}} = \frac{C_0 V_{DC} \gamma_L A_1 I V_{bias}}{G m_e t w_g} \frac{1}{\Omega_1^2 - \omega^2 + j \frac{\omega \Omega_1}{Q}}, \quad (4)$$

where  $V_{bias}$  is the bias voltage applied to the gauge.

The NEMS behaves as a bandpass filter with a high quality factor. At resonance ( $\omega = \Omega_1$ ), its gain  $g_{nems}$  and phase  $\psi_{nems}$  are equal to:

$$g_{nems} = \frac{C_0 V_{DC} \gamma_L A_1 I V_{bias}}{G m_e t w_g} \frac{Q}{\Omega_1^2}, \quad (5)$$

$$\psi_{nems} = -\pi / 2. \quad (6)$$

In a properly designed system, the beam should oscillate at a frequency close to  $\Omega_1$ . To determine with accuracy the oscillator behavior close to its working frequency, one can compute the Taylor expansion of  $H_{nems}$  when  $\omega$  is close to  $\Omega_1$ . This yields:

$$G_{nems} = \frac{C_0 V_{DC} \gamma_L A_1 I V_{bias}}{G m_e t w_g} \frac{Q}{\Omega_1^2} \frac{1/\Omega_1^2}{4 \frac{\omega - \Omega_1}{\Omega_1} + \frac{1}{Q^2}} \quad (7)$$

$$\approx g_{nems} \left( 1 - 2Q^2 \frac{\omega - \Omega_1}{\Omega_1} \right), \quad (8)$$

$$\psi_{elec} = -\arg \left( \Omega_1^2 - \omega^2 + j \frac{\omega \Omega_1}{Q} \right) = -\pi / 2 - 2Q \frac{\omega - \Omega_1}{\Omega_1}, \quad (9)$$

where  $G_{nems}(\omega)$  and  $\Psi_{nems}(\omega)$  are the amplitude and phase responses of the NEMS. Equations (8) and (9) lead to:

$$G_{nems} = g_{nems} \left[ 1 - \frac{\pi / 2 + \psi_{nems}}{2} \right], \quad (10)$$

Note that, because of the large value of  $Q$ ,  $\psi_{elec}$  can be fairly different from  $-\pi/2$  and  $\omega$  still be very close to  $\Omega_1$ .

### B. Oscillation conditions

To determine the oscillation conditions of a closed-loop system, one must consider the open loop transfer function  $H_{OL}$  of the NEMS and its electronic.  $H_{OL}$  is the product of the transfer function of the NEMS and that of the sustaining electronic  $H_{elec}$ . The output voltage of the electronic circuit is called  $V_{elec}$ .  $v_{elec}$  is its AC component. In the closed-loop configuration,  $V_{elec}$  is applied to the actuation electrode of the NEMS ( $V_{elec} = V_{in}$ ). According to the Barkhausen criterion, oscillations start building up when

$$\text{Re}(H_{nems} \times H_{elec}) > 1 \text{ and } \text{Im}(H_{nems} \times H_{elec}) = 0, \quad (11)$$

and stabilize when

$$H_{nems} \times H_{elec} = 1. \quad (12)$$

The electronic feedback circuit must amplify and shift the phase of  $v_{nems}$  in order for the open-loop transfer function to satisfy the Barkhausen criterion. From (5) and (6),  $H_{elec} = v_{elec} / v_{beam}$  must have a gain superior to  $1/g_{nems}$  and a phase of  $\psi_{elec} = \pi/2$  to ensure oscillation at  $\Omega_1$ . If  $\psi_{elec}$  is different from  $\pi/2$ , the system starts oscillating at the frequency for which  $\psi_{nems} = -\psi_{elec}$  if  $|H_{nems} H_{elec}| \geq 1$ . In this

case, the minimum electronic gain can be determined from equation (10):

$$G_{elec-min} = \frac{1}{g_{nems} \left( 1 - \frac{\pi/2 - \psi_{elec}}{2} \right)}. \quad (13)$$

Once the oscillation builds up, one must control their amplitude. One possible approach consists in dynamically adapting the electronic gain through an automatic gain control (AGC) so that  $|H_{nems}H_{elec}|=1$ . In our approach, the intrinsic nonlinearities of the electronic circuit are used to stabilize the oscillation at a desired amplitude, without the need of an AGC. However, this approach requires special attention in the design of the electronics to ensure the functionality of the whole system.

### C. Design of the feedback electronic

As exposed in sub-section B,  $H_{elec}=v_{elec}/v_{beam}$  must have a phase close to  $\pi/2$  and a gain greater than  $1/g_{nems}$  close to the NEMS natural frequency.

The schematic of the electronics is shown in fig. 1. The voltage  $v_{beam}$  is amplified and converted into a current through the active transistor  $M_0$ . This current flows into the output capacitor  $C_{out}$  to compensate the overall phase.

The gate of  $M_0$  is polarized through the piezoresistive gauge of the NEMS. The transistor  $M_p$  polarized by  $V_b$  acts as a current source which polarizes  $M_0$ . In order to achieve a large  $g_{nems}$ ,  $V_{DC}$  should be as large as possible. Since  $V_{DC}$  is the DC component of  $V_{nems}-V_{elec}$ , caution must be taken while designing  $M_0$  to ensure a DC operating point  $V_{elec}$  as small as possible.

The small signal transfer function of the electronic circuit is:

$$H_{elec} = \frac{-g_m}{g_{ds0} + g_{dsP} + j\omega(C_{out} + C_{db0} + C_{dbP} + C_{dgP})}, \quad (14)$$

where  $g_m$ ,  $g_{ds}$ ,  $C_{db}$ ,  $C_{dg}$  are respectively the transconductance, the transimpedance, the drain-bulk capacitance and the drain-gate capacitance of the transistors (the indices 0 and P designate  $M_0$  and  $M_p$ ). Let  $C_{load} = C_{out} + C_{db0} + C_{dbP} + C_{dgP}$  and  $g_{ds0}$ ,  $g_{dsP} \ll \omega C_{load}$ , the transfer function of the electronic becomes:

$$H_{elec} \approx \frac{-g_m}{j\omega C_{load}}. \quad (15)$$

Thus the phase of  $H_{elec}$  is approximately  $\pi/2$ , which satisfies (11) if the gain is sufficient.

Using a CMOS 0.13 $\mu$ m technology from ST Microelectronics (HCMOS9GP\_9.2) for which  $V_{dd}=1.2V$ , the dimensions of  $M_0$  and  $M_p$  in fig. 1 and  $V_b=0.45V$  the following values are extracted:

$$\begin{array}{lll} g_m=163\mu S & g_{ds0}=25\mu S & C_{db0}=1.3fF \\ C_{gs0}=8.8fF & C_{gb0}=0.6fF & C_{dbP}=1.3fF \\ g_{dsP}=0.4\mu S & C_{dbP}=3.5fF & C_{dgP}=3.2fF \end{array} \quad (16)$$

These values lead to an input admittance of  $Y_{in}=6.9\mu S \ll 1/R_0=727\mu S$  at  $\Omega_1$  (which confirms the assumption made where the input electronic impedance is huge compared to  $R_0$ ) and to an electronic transfer function characteristics at  $f_i=50MHz$ :

$$G_{elec}=2.9 \quad \psi_{elec}=2.0rad \approx 117^\circ. \quad (17)$$

The DC component of  $V_{elec}$  is 0.24V which leads to

$V_{DC}=0.36V$ . From (5), this results in  $1/g_{nems}=2.2$ . Close to  $\Omega_1$  the electronic gain is thus larger than the minimal value  $G_{elec-min}=2.45$  imposed by (10). The system should therefore start oscillating.

### III. AMPLITUDE OF THE STABLE OSCILLATIONS

As described in section II, the stabilization of the oscillation amplitude is achieved thanks to the nonlinear behavior of the electronic circuit. In order to establish the steady-state amplitude of  $v_{beam}$ , the describing function gain [7] of the electronic circuit must be determined. A series of transient simulations of the circuit behavior under a wide range of values of  $v_{beam}$  is then performed with SPICE. Assuming that  $H_{elec}$  is locally independent of  $\omega$  close to  $\Omega_1$ , the pulsation is set to  $\Omega_1$  and the DC input voltage to  $V_{dd}/2$ . The DC and AC components of  $V_{elec}$  are then determined through Fourier analysis. The resulting evolution of  $G_{elec}$ ,  $\psi_{elec}$  and of the DC component of  $V_{elec}$  is represented in fig. 2. For low values of  $v_{beam}$ ,  $G_{elec}$  is larger than what is predicted in section II.C (this is due to the fact that the models used for the small-signal analysis are less accurate than those used for the transient simulation) and the other quantities are close to the expected ones: the system should then start oscillating. Because the value of the DC component of  $V_{elec}$  is small, the electronic circuit has a low output dynamic range. Thus, as  $v_{beam}$  increases,  $V_{elec}$  is more and more distorted, which results in an increase of its DC component. For larger values of  $v_{beam}$ ,  $G_{elec}$  starts to decrease. Thus, as the oscillation builds up, two effects add up. First, the DC component of  $V_{elec}$  increases, which makes  $V_{DC}$  decrease and, consequently,  $g_{nems}$  and  $G_{nems}$ . Furthermore  $G_{elec}$  decreases. Therefore, starting from a value of  $G_{nems} \times G_{elec}$  superior to 1, the system should stabilize provided  $G_{nems}$  and  $G_{elec}$  decrease sufficiently.

Knowing  $g_{nems}(v_{beam})$  and  $\psi_{elec}(v_{beam})$  and using (10), one may then plot  $G_{nems}$  vs.  $v_{beam}$  using the fact that, in the steady-state,  $\psi_{nems}$  should be equal to  $-\psi_{elec}$ . The existence of a steady-state regime can then be determined from the intersection of  $G_{nems}(v_{beam})$  and  $1/G_{elec}(v_{beam})$  (fig. 3). The intersection corresponds to a stable displacement amplitude of the beam of about 4nm (validating the hypothesis done in section II.A:  $y \ll \langle G \rangle$ ) and to an electronic phase-shift of  $\psi_{elec}=117^\circ$ . From (9), we find  $(\omega - \Omega_1)/\Omega_1 \approx 2.4 \times 10^{-4}$  which confirms the hypothesis  $\omega \approx \Omega_1$  made in this paper. The corresponding AC voltage at the input of the NEMS is  $v_{in} \approx 210mV$ .

Finally, a transient simulation of the complete system is performed. The NEMS is modeled with a VHDL-AMS description based on [8]. The evolution of the envelope of  $y$  vs. time is plotted in fig. 4. The steady-state mechanical oscillation amplitude is equal to 3.8nm, which corresponds to an electronic output voltage of 203mV. These results validate the proposed design approach.

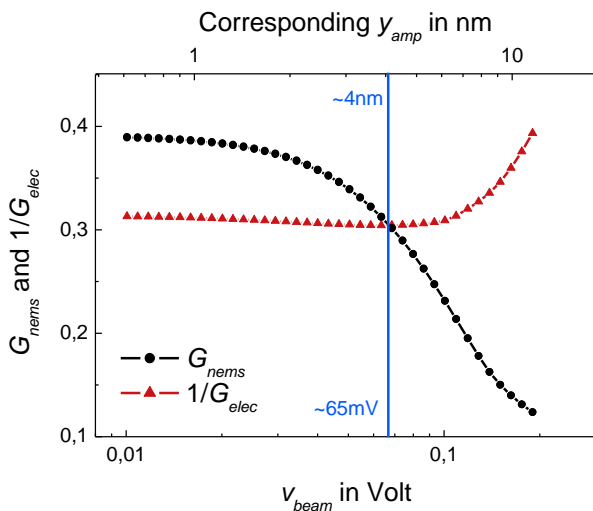


Fig. 3. Evolution of  $G_{nems}$  and  $1/G_{elec}$  with  $v_{beam}$  at  $\psi_{elec} = -\psi_{nems}$

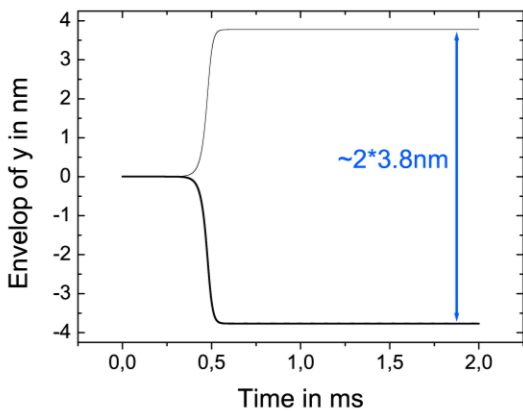


Fig. 4. Evolution of the envelop of  $y$  with time calculated through a SPICE/VHDL-AMS simulation.

#### IV. CONCLUSION

In this paper, the design of a NEMS/CMOS oscillator was presented. The behavior of the resonator was first described in terms of phase and gain and its oscillation conditions were established. An electronic circuit was then designed to fulfill these conditions. We showed that the electronic part of the system can be designed so that stable oscillations can be obtained through the intrinsic nonlinearity of the electronic part. This method provides a very simple procedure to design an oscillator with a given mechanical displacement without the need of an automatic amplitude control. The proposed architecture is so compact that it can be implemented with ease in a sensor array application, for example.

#### REFERENCES

- [1] B. Borovic, C. Hong, X.M. Zhang, A.Q. Liu, and F.L. Lewis, "Open vs. closed-loop control of the MEMS electrostatic comb drive," in *Proc. IEEE International Symposium on Mediterrean Conference on Control and Automation Intelligent Control*, pp. 982–988, 2005.
- [2] K.L. Ekinici, "NEMS: All you need is feedback," *NATURE NANOTECHNOLOGY*, vol. 3, pp. 319–320, JUN 2008.
- [3] O. Brand, "Microsensor integration into systems-on-chip," vol. 94, pp. 1160–1176, June 2006.
- [4] J. Arcamone, B. Mischischi, F. Serra-Graells, M.A.F. van den Boogaart, J. Brugger, F. Torres, G. Abadal, N. Barniol, and F. Perez-Murano, "Compact CMOS current conveyor for integrated NEMS resonators," *IET Circuits, Devices & Systems*, vol. 2, pp. 317–323, June 2008.

- [5] J. Verd, A. Uranga, J. Teva, J.L. Lopez, F. Torres, J. Esteve, G. Abadal, F. Perez-Murano, and N. Barniol, "Integrated CMOS-MEMS with on-chip readout electronics for high-frequency applications," vol. 27, no. 6, pp. 495–497, 2006.
- [6] L. He, Y.P. Xu, and M. Palaniapan, "A CMOS readout circuit for SOI resonant accelerometer with 4- $\mu$ g bias stability and 20- $\mu$ g/ $\sqrt{\text{Hz}}$  resolution," vol. 43, no. 6, pp. 1480–1490, 2008.
- [7] A. Gelb and W. Van der Velde, *Multiple-input describing functions and nonlinear system design*. McGraw-Hill, New-York, 1968.
- [8] E. Colinet, L. Duraffourg, S. Labarthe, S. Hentz, P. Robert, and P. Andreucci, "Self-oscillation conditions of a resonant nanoelectromechanical mass sensor," *Journal of Applied Physics*, vol. 105, no. 12, pp. 124908–8, 2009.
- [9] Y. Yang, C. Callegari, X. Feng, K. Ekinici, and M. Roukes, "Zeptogram-scale nanomechanical mass sensing," *NANO LETTERS*, vol. 6, pp. 583–586, APR 2006.